Ripple-free Control Response by Using a Fractional Order Hold Device

Unai Ugalde, Rafael Bárcena, Koldo Basterretxea
Department of Electronics and Telecommunications
University of the Basque Country
La Casilla, 3. 48012 Bilbao.
SPAIN
unai.ugalde@ehu.es http://www.ehu.es/jtpugolu

Abstract: In digital control, discrete-time signal reconstruction is usualy carried out by the zero-order hold (ZOH), although other options exist which exhibit interesting properties. A remarkable alternative is the fractional-order hold (FROH), which provokes no intersample ripple under steady state and, if properly tuned, can often place the discretized plant model *z*-domain zeros in more convenient locations than the ZOH. This zero placing technique, in turn, gives rise to closed-loop performance improvements for many cases. However, since it is formulated in the *z*-domain, it cannot anticipate continuous-time closed-loop behaviour. Besides, going through zero placement is burdensome, especially for high-order models. This work presents a new and simpler method which directly links the tuning of the FROH with some desired closed-loop features, bypassing zero placement. It is based on the frequency domain, which makes it possible to capture the continuous-time behaviour. The simulations performed have shown clear improvements over zero placement, in terms of time-domain performance figures, intersample behaviour, and the energy consumed in step responses.

Key-Words: Frequency domain analysis, Sampled data systems, Digital control.

1 Introduction

In digital control, discrete-time signal reconstruction is usualy carried out by the zero-order hold (ZOH) [9, 14, 16]. However, since the zeros of the discretized model of a linear, time-invariant, continuous-time plant depend on the hold device, many authors call for the use of alternative reconstruction strategies. Among these is the fractional-order hold (FROH), which provokes no intersample ripple under steady state and, if properly tuned, can place such *z*-domain zeros closer to the origin than the ZOH can, for a wide range of plants and sampling rates [12, 15]. This last fact is very attractive for some *z*-domain controller design methods, particularly those involving zero cancellation. On the other hand, discretization zeros (i.e. those not having continuous-time counterparts) tend to be located on the negative real axis, and cancelling these zeros always involves intersample ripple to some extent [1, 17]. Therefore, several works deal with locating the zeros in positions which give the best discrete-time performance (for a given set of closed-loop poles) [3–7].

Nevertheless, this approach does not capture the intersample behaviour. Hence, one must either rely on *a posteriori* simulations so as to verify that the intersample is well behaved, or assume fast sampling (relative to the closed-loop bandwith). Obviously, the improvements that alternative reconstruction strategies may produce will tend to vanish as the reconstruction period diminishes, so in practice one must perform such simulations, and be ready to go back to the drawing board if the results do not come up to expectations. And anyway a method would be desirable that avoided to go through the tedious and time-consuming zero-placement procedures.

Therefore, we will take another approach. It will consist on relating the tuning of the FROH directly with the continuous-time closed-loop performance. Thus the issue of *z*-domain zero placing will not play a central role, nor will be our aim to cancel these zeros (in fact, we will consider the more realistic option of always transferring them). To this aim, we will base our analysis on the frequency domain; in particular, we will use [11, Ch. 14] as our starting point. There, the authors introduce a function that captures the relationship between the continuous-time response (i.e. the actual one) and the sampled-and-held –via a ZOH– fictitious response (i.e. a reasonable extrapolation of what the controller sees). Basically, we will use the ability to shape this relationship that the FROH posesses (through its scalar gain β), in order to "recover" closed-loop performance at the damped frequency. The simulations performed have shown clear improvements over the traditional *z*-domain zero placing technique, in terms of time-domain performance figures, intersample behaviour, and the energy consumed in step responses.

For the sake of simplicity, we will restrict ourselves to single-input, single-output systems. Also, we will use the well-known 2-degree-of-freedom ("RST") digital controller, adjusted to obtain a pair of pre-specified dominant closed-loop poles ("pole placement") [2, Ch. 5].

2 The Fractional-order Hold in the Frequency Domain

2.1 Fractional-order hold preliminaries

Given a discrete-time signal $u[k]$ (usually, emerging from a digital controller), the FROH-reconstructed continuous-time signal $v(t)$ (usually, driving a plant input) is [15, 8]

$$v(t) = u[k] + \beta \frac{u[k] - u[k-1]}{h}(t - kh),\ t \in [kh, h) \quad (1)$$

where h is the sampling period under which the digital controller operates, and β is an adjustable parameter, whose value is to be determined by the tuning method. The impulse response corresponding to (1) is

$$G_{\mathrm{FROH}}(s) = G_{\mathrm{ZOH}}(s)\left(1 + \beta \frac{1 - \mathrm{e}^{-sh}(1 + sh)}{sh}\right), \quad (2)$$

where

$$G_{\mathrm{ZOH}}(s) = \frac{1 - \mathrm{e}^{-sh}}{s}. \quad (3)$$

There are two well-known properties relating FROH-discretized to ZOH-discretized plant models. Let us respectively denote them by

$$[GG_{FROH}](z) = \frac{B_{FROH}(z)}{A_{FROH}(z)} \quad (4)$$

$$[GG_{ZOH}](z) = \frac{B_{ZOH}(z)}{A_{ZOH}(z)}, \quad (5)$$

whose denominators are monic but not necessarily their numerators. Then we have that [15]

$$A_{FROH}(z) = z\, A_{ZOH}(z), \quad (6)$$

from which $A_{\mathrm{FROH}}(1) = A_{\mathrm{ZOH}}(1)$, as well as that

$$B_{FROH}(1) = B_{ZOH}(1), \quad (7)$$

because of (6) and the fact that static gain is preserved, i.e. $[GG_{\mathrm{FROH}}](1) = [GG_{\mathrm{ZOH}}](1)$. Equation (6) also allows us to drop the subscripts of the denominators, so we will write $A_{\mathrm{ZOH}} \equiv A$ and $A_{\mathrm{FROH}} \equiv z \cdot A$ in the sequel.

2.2 Continuous-time vs. discrete-time response

In a closed-loop digital control sheme, where a ZOH performs the discrete-to-continuous reconstruction, the relationship between the continuous-time real output and a sampled-and-held (via ZOH) fictitious output is [11, Ch. 14]

$$\Theta(s) \triangleq \frac{y_{\mathrm{ZOH}}(s)}{\bar{y}_{\mathrm{ZOH}}(s)} = \frac{G(s)}{[GG_{\mathrm{ZOH}}](\mathrm{e}^{sh})} = \frac{N(s)A(\mathrm{e}^{sh})}{D(s)B_{ZOH}(\mathrm{e}^{sh})}, \quad (8)$$

where $N(s)$ and $D(s)$ are, respectively, the numerator and denominator of the continuous-time plant model.

In short, $\Theta(j\omega)$ provides information on how near or far the real response and the sampled (and 'ZOH-ed') response are from each other at the frequency ω. For example, if there are z-domain zeros on (or near) the negative real axis, we can expect $|\Theta(j\omega)|$ to have a large peak at (or about) the Nyquist frequency $\omega_{\mathrm{N}} = \pi/h$. This will likely be the case if those zeros are discretization zeros (indeed, *will* tend to be the case as $h \to 0$) [1]. So one usually tries to push ω_{N} away from the frequencies of interest (for example, the damped closed-loop frequency ω_{d}; i.e, the one with which the transients oscillate) either by decreasing h or by limiting the achievable bandwith [11, Ch. 14] — the well-established "bandwidth × sampling period" trade-off [10, 11, 13].

However, let us turn our attention to the FROH in order to get more insight into the matter, by relating the continuous-time closed-loop responses of the ZOH and FROH cases. To begin with, we will derive an expression equivalent to (8) for the FROH case:

$$\Theta_{\mathrm{FROH}}(s) \triangleq \frac{y_{\mathrm{FROH}}(s)}{\bar{y}_{\mathrm{FROH}}(s)} = \frac{N(s)\mathrm{e}^{sh}A(\mathrm{e}^{sh})}{D(s)B_{\mathrm{FROH}}(\mathrm{e}^{sh})}\frac{G_{\mathrm{FROH}}(s)}{G_{\mathrm{ZOH}}(s)}. \quad (9)$$

Note that although a FROH is used to reconstruct the control signal in (9), a ZOH is again –as in (8)– used to reconstruct the fictitious sampled output.

Next, let us tune two RST controllers (one for each case) to achieve the same closed-loop poles. If we do not cancel zeros in either case, then the closed-loop *z*-domain transfer functions become

$$H_{\mathrm{FROH}}(z)=\frac{A'(1)}{B_{\mathrm{FROH}}(1)}\frac{B_{\mathrm{FROH}}(z)}{z\,A'(z)} \tag{10}$$

$$H_{\mathrm{ZOH}}(z)=\frac{A'(1)}{B_{\mathrm{ZOH}}(1)}\frac{B_{\mathrm{ZOH}}(z)}{A'(z)} \tag{11}$$

where $A'(z)$ is a polynomial whose degree is equal to that of $A(z)$, and typically has a pair of dominant roots. In view of (6), it is obvious that (10) will have one more pole than (11), which we have chosen to be at the origin. Besides, according to (7), both constant terms in (10)–(11) are equal.

These last considerations and equations (8)–(11) allow us to infer the relation between the continuous outputs of both cases as

$$\begin{aligned}\frac{y_{\mathrm{FROH}}(s)}{y_{\mathrm{ZOH}}(s)}&=\frac{\Theta_{\mathrm{FROH}}(s)}{\Theta(s)}\frac{\bar{y}_{\mathrm{FROH}}(s)}{\bar{y}_{\mathrm{ZOH}}(s)}\\&=\frac{\dfrac{N(s)\mathrm{e}^{sT}A(\mathrm{e}^{sh})G_{\mathrm{FROH}}(s)}{D(s)B_{\mathrm{FROH}}(\mathrm{e}^{sh})G_{\mathrm{ZOH}}(s)}\dfrac{B_{\mathrm{FROH}}(\mathrm{e}^{sh})}{\mathrm{e}^{sT}A'(\mathrm{e}^{sh})}}{\dfrac{N(s)A(\mathrm{e}^{sh})}{D(s)B_{\mathrm{ZOH}}(\mathrm{e}^{sh})}\dfrac{B_{\mathrm{ZOH}}(\mathrm{e}^{sh})}{A'(\mathrm{e}^{sh})}}\\&=\frac{G_{\mathrm{FROH}}(s)}{G_{\mathrm{ZOH}}(s)},\end{aligned} \tag{12}$$

which holds for any input. Finally, with the help of (2), equation (12) becomes

$$\frac{y_{\mathrm{FROH}}(s)}{y_{\mathrm{ZOH}}(s)}=1+\beta\frac{1-\mathrm{e}^{-sh}(1+sh)}{sh}\triangleq\Psi(sh). \tag{13}$$

Thus $\psi(\mathrm{j}\omega h)$ represents how near or far the *continuous-time* responses that (10)–(11) give rise to are from each other at the frequency ω. Also, from (8) and (13) we get

$$y_{\mathrm{FROH}}(s)=\Psi(sh)\,y_{\mathrm{ZOH}}(s)=\Psi(sh)\Theta(s)\bar{y}_{\mathrm{ZOH}}(s) \tag{14}$$

Therefore, whenever we expect a $y_{\mathrm{ZOH}}(s)$ significantly different than the corresponding $\bar{y}_{\mathrm{ZOH}}(s)$, we may switch to a FROH tuned according to a desired $\psi(sh)$ that yields a better $y_{\mathrm{FROH}}(s)$.

2.3 Performance recovery at the damped frequency under slow sampling

As was pointed out earlier, it is common to have *z*-domain zeros on or near the negative real axis. If additionaly one has to operate a loop near the Nyquist frequency, one must expect an undesirable $y_{\mathrm{ZOH}}(\mathrm{j}\omega_{\mathrm{d}})$, as $|\Theta(\mathrm{j}\omega_{\mathrm{d}})|$ will be high because of the peak of $|\Theta(\mathrm{j}\omega_{\mathrm{N}})|$. This foresees e.g. a continuous-time overshoot much higher than the discrete-time one.

However, if we choose a β value in (13) such that

$$\left|\Psi(\mathrm{j}\omega_{\mathrm{d}}h)\right|^2=\frac{1}{\left|\Theta(\mathrm{j}\omega_{\mathrm{d}})\right|^2}, \tag{15}$$

then

$$\left|y_{\mathrm{FROH}}(\mathrm{j}\omega_{\mathrm{d}})\right|=\frac{1}{\left|\Theta(\mathrm{j}\omega_{\mathrm{d}})\right|}\left|y_{\mathrm{ZOH}}(\mathrm{j}\omega_{\mathrm{d}})\right|=\left|\bar{y}_{\mathrm{ZOH}}(\mathrm{j}\omega_{\mathrm{d}})\right| \tag{16}$$

and the magnitude of the continuous-time response of the FROH case at ω_{d} will be the same as the magnitude of the discrete-time ZOH case at ω_{d}.

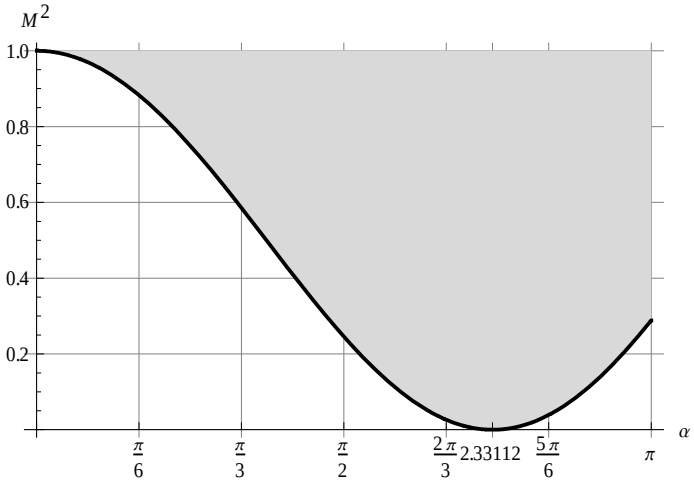

Figure 1. Region on the ($\omega_{\mathrm{d}}h$, M^2) plane where β is real valued (up to the Nyquist frequency $\omega_{\mathrm{N}}h=\pi$).

For the sake of clarity, let us introduce $\alpha \equiv \omega h$ and $M \equiv 1/|\Theta(j\omega_d)|$, where $M < 1$ typically. Then, it is straightforward to show that (15) can be rewritten as

$$\left(1+2\frac{1-\cos\alpha}{\alpha^2}-2\frac{\sin\alpha}{\alpha}\right)\beta^2-2\left(\cos\alpha-\frac{\sin\alpha}{\alpha}\right)\beta=M^2-1 \tag{17}$$

Thus, to have real-valued solutions (discriminant ≥ 0), M^2 must belong to the shaded region of Fig. 1. Slow sampling means ω_d close to ω_N; therefore, we can expect real solutions for many cases.

In such instances, one solves (17) and gets two real values for β. To help choose one of them, we will turn our attention to the phase of $\psi(j\omega_d h)$, and will take the β that gives less absolute phase, with perhaps some phase advance.

3 Application Examples

In the following, we will illustrate the benefits of our new method through two examples. In each and every case, a RST digital controller [2] will have been tuned to obtain the same closed-loop denominator in the *z*-domain. This means a pair of dominant poles, and as many as needed "padding" poles at the origin; also recall (10)–(11). As to the *z*-domain plant zeros, they will always be transferred, so the only reason why we will have to care about their positions is to tune the corresponding controller.

In short, as long as controller tuning is concerned, we will proceed as follows. Given a ZOH-discretized plant model (4) or a FROH-discretized plant model (5), the following Diophantine equation arises (we will drop the subindices whenever they are irrelevant)

$$A(z)R(z)+B(z)S(z)=A'(z), \tag{18}$$

where $A'(z)$ captures the desired closed-loop dynamics, so one must determine the required $R(z)$, $S(z)$ pair so as to obtain certain pre-specified $A'(z)$.

As is usual [2], we will factor $A'(z)$ into a "controller" polynomial, whose degree is equal to that of $A(z)$, and an "observer" polynomial, i.e.

$$A'(z)=A'_c(z)A'_o(z). \tag{19}$$

On the one hand, the roots of the controller polynomial $A'_c(z)$ become the closed-loop poles, which we will choose to be a dominant pair, plus as many poles at the origin as needed, to reach the degree of $A(z)$.

On the other hand, the roots of the "observer" polynomial $A'_o(z)$, which are to be cancelled by $T(z)$, will all be chosen to lie at the origin — this is why $T(z)$ will adopt a monomial form in all instances of the following examples.

3.1 A simple case

This example compares the closed-loop responses of two cases: a FROH tuned according to the "traditional" zero-placing procedure ("FROH1 case") as well as a FROH tuned according to the method being introduced here ("FROH2" case). In addition, we will first consider the ZOH case, just for reference; i.e. we do not intend to compare FROH with ZOH performance improvements (though there *will* be improvements, naturally).

Let us take a simple model like

$$G(s)=\frac{1}{s(s+1)}. \tag{20}$$

It has one ZOH-discretization zero which, being the only zero, must be real. Also, if we take the sampling period as

$$h=0.1\,\mathrm{s}, \tag{21}$$

then $\omega_N = 31.4159$ rad s^{-1} and it turns out that $|\Theta|$ has the considerable peak of $|\Theta(j\omega_N)| = 24.3291$ at the Nyquist frequency (more on this later).

As to the closed-loop dynamics, we will take a pair of dominant poles given by a natural frequency of

$$\omega_0=30\ \mathrm{rad\ s^{-1}} \tag{22}$$

and a damping of

$$\zeta=0.5, \tag{23}$$

which give a damped frequency of

$$\omega_d=25.9808\ \mathrm{rads^{-1}}. \tag{24}$$

First, with a ZOH, we obtain the following z-domain plant model, controller polynomials and closed-loop z-domain response

$$\left[GG_{\mathrm{ZOH}}\right](z)=\frac{0.0048374(z+0.9672)}{(z-1)(z-0.9048)} \quad , \tag{25}$$

$$\begin{cases} R_{\mathrm{ZOH}}(z)=z+0.8055 \\ S_{\mathrm{ZOH}}(z)=306.2211z-155.7692 \\ T_{\mathrm{ZOH}}(z)=150.4519z \end{cases} , \tag{26}$$

$$H_{\mathrm{ZOH}}(z)=\frac{0.7278\ (z+0.9672)}{\left(z^2+0.382z+0.04979\right)} \quad . \tag{27}$$

Next, we will consider the FROH1 case. Since the relative order (pole-zero excess) of (20) is $p = 2$, we can apply [4]. Thus, seeking a double real z-domain zero, we take $\beta = -0.32505484$, which gives rise to

$$\left[GG_{\mathrm{FROH1}}\right](z)=\frac{0.0043089(z+0.4861)^2}{z(z-1)(z-0.9048)} \quad , \tag{28}$$

$$\begin{cases} R_{\mathrm{FROH1}}(z)=z^2+0.8055z+0.1998 \\ S_{\mathrm{FROH1}}(z)=327.9958z^2-177.5439z \\ T_{\mathrm{FROH1}}(z)=150.4519z^2 \end{cases} , \tag{29}$$

$$H_{\mathrm{FROH1}}(z)=\frac{0.64289\ (z+0.4861)^2}{z\left(z^2+0.382z+0.04979\right)} \quad . \tag{30}$$

Last, let us deal with the FROH2 case. Since it turns out that

$$\left|\Theta\left(\mathrm{j}\omega_{\mathrm{d}}\right)\right|=2.04533\,, \tag{31}$$

recalling (15) and (21)–(24) we seek a β such that

$$M^2=\left|\Psi\left(\mathrm{j}2.59808\right)\right|^2=\frac{1}{(2.04533)^2}=0.23904\,. \tag{32}$$

Now (17) takes the form

$$1.5179\beta^2+2.10989\beta+0.760958=0\,, \tag{33}$$

whose roots are

$$\begin{cases} \beta_1=-0.493743 \\ \beta_2=-1.33809 \end{cases} . \tag{34}$$

Figs. 2 and 3 show $|\Theta|$, $|\psi|$ as well as their product, all versus ω, for β_1 and β_2 respectively. Both figures show that $|\Theta| = 2.04533$ and $|\Theta\psi| = 1$ at ω_d. Likewise, Figs. 4 and 5 show the corresponding phase responses. Observe that β_1 intoduces a small phase lead at ω_d, whereas β_2 introduces a significant phase lag at ω_d; in view of this, we will take $\beta = \beta_1$.

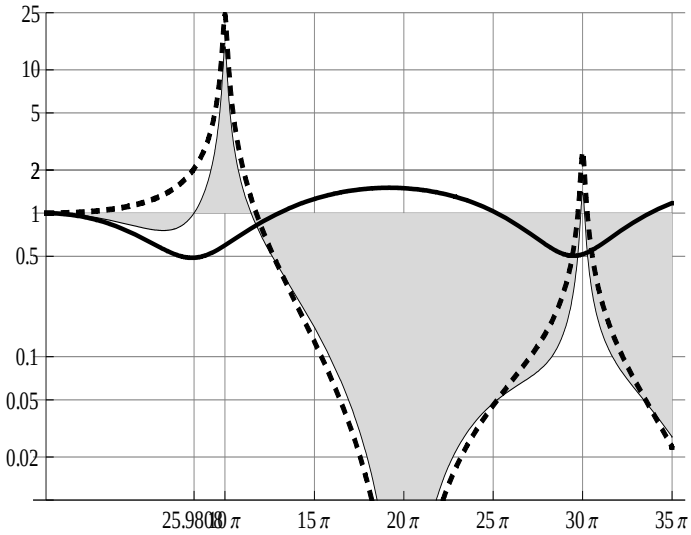

Figure 2. $|\Theta|$ (dashed), $|\psi|$ (thick) and $|\Theta\psi|$ (filled) for β_1.

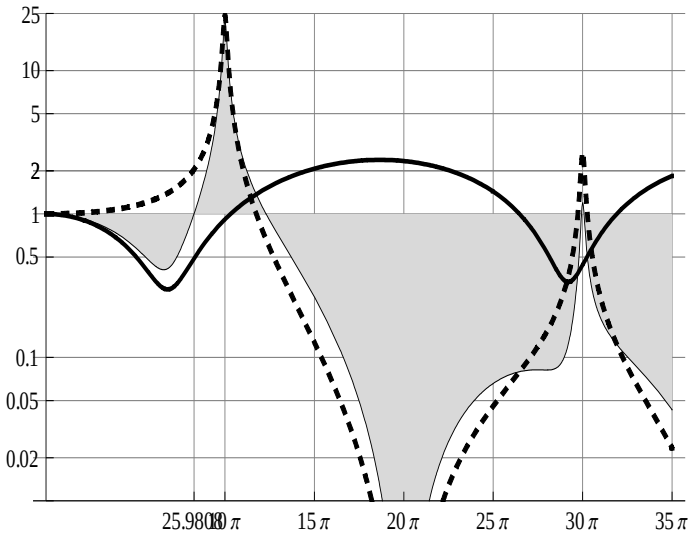

Figure 3. $|\Theta|$ (dashed), $|\psi|$ (thick) and $|\Theta\psi|$ (filled) for β_2.

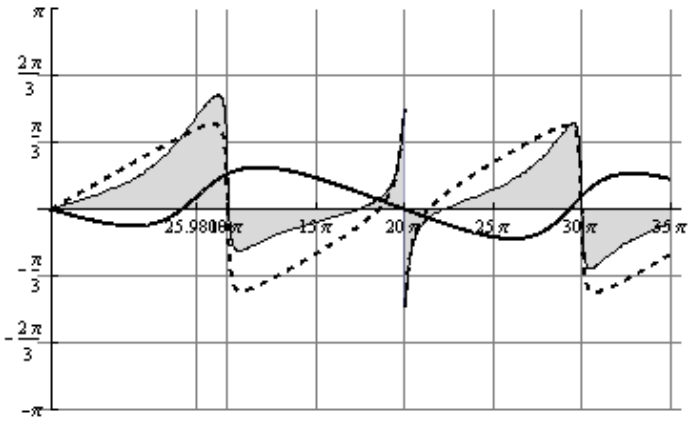

Figure 4. Phase responses corresponding to Fig. 2.

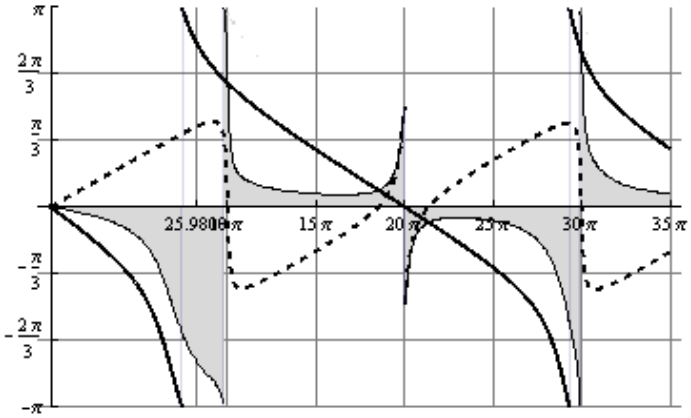

Figure 5. Phase responses corresponding to Fig. 3.

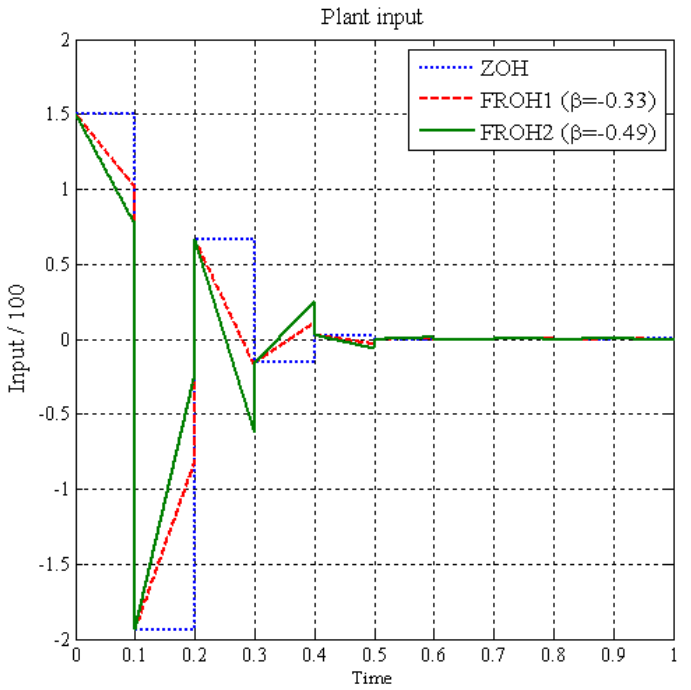

Figure 6. Plant input. ZOH (dotted), FROH1 (dashed), FROH2 (solid).

Then, the resulting relevant expressions are:

$$\left[GG_{\text{FROH2}}\right](z)=\frac{0.0040347\left(z^2+0.9753z+0.3833\right)}{z\left(z-1\right)\left(z-0.9048\right)} \tag{35}$$

$$\begin{cases} R_{\text{FROH2}}(z)=z^2+0.9190z+0.3223 \\ S_{\text{FROH2}}(z)=339.0053z^2-188.5534z \\ T_{\text{FROH2}}(z)=150.4519z^2 \end{cases} \tag{36}$$

$$H_{\text{FROH2}}(z)=\frac{0.60703\left(z^2+0.9753z+0.3833\right)}{z\left(z^2+0.382z+0.04979\right)} \tag{37}$$

Fig. 6 (plant input) and Fig. 7 (plant output) show the step responses of the three cases studied. Table 1 shows some significant performance figures, such as settling time (5% criterion), overshoot and energy consumed during the transient.

Figure	ZOH	FROH1	FROH2
$t_{s,5\%}$	296 ms	189 ms	160 ms
OS	23.25%	5.80%	3.31%
Energy	6479	3732	2906

Table 1. Significant performance figures.

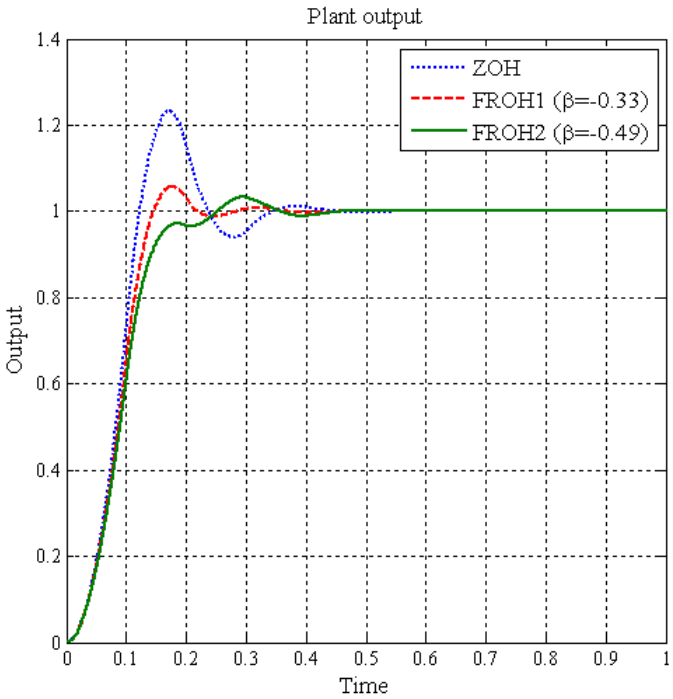

Figure 7. Plant output. ZOH (dotted), FROH1 (dashed), FROH2 (solid).

Table 1 makes it clear that both FROHs deliver better performance that the ZOH. Nevertheless, as to the FROHs themselves, the best results are given by the new method introduced in this work, not only in terms of the preformance figures, but also considering the continuous-time output. Indeed, Figure 7 shows that the output signal corresponding to the new method has a much smoother continuous-time response, in the sense that the intersample values tend to lie between the at-sample values. This is by no means true of the FROH tuned according to the traditional method; e.g., a pure *z*-domain analysis would not anticipate its continuous-time overshoot, so one might tune the FROH in the *z*-domain to optimize this or other performance figure, only to see in *a posteriori* simulations that things are not actually what they seemed to be.

3.2 A higher-order plant

This second example compares the closed-loop responses of a FROH tuned according to our new method and the ZOH case. Indeed, we cannot apply the "traditional" method of [4], bacause it may only be applied to a relative order $p = 2$, and this example considers a case whose $p = 4$ (see below). On the other hand, we will keep the sampling rate and closed-loop desired dynamics of the first example; that is, (21)–(24) will also apply to this second example.

So, now we turn to a higher-order model such as

$$G(s) = \frac{100}{s\left(s^3 + 19.9s^2 + 98.25s - 10.025\right)}, \qquad (38)$$

which has a pair of complex-conjugate poles at –10±j0.5 and one unstable pole at +0.1.

First, with a ZOH, we obtain the following *z*-domain plant model, controller polynomials and closed-loop *z*-domain response:

$$\left[GG_{\text{ZOH}}\right](z) = \frac{0.00028541\left(z + 6.894\right)\left(z + 0.6727\right)\left(z + 0.06539\right)}{\left(z - 1\right)\left(z^3 - 1.7449z^2 + 0.8776z + 0.1367\right)} \qquad (39)$$

$$\begin{cases} R_{\text{ZOH}}(z) = z^3 + 2.6275z^2 + 1.4568z + 0.0843 \\ S_{\text{ZOH}}(z) = 1749.5z^3 - 2200.3z^2 + 940.6z - 133.2 \\ T_{\text{ZOH}}(z) = 356.5964z^3 \end{cases} \qquad (40)$$

$$H_{\text{ZOH}}(z) = 0.10178\frac{(z + 6.894)\ (z + 0.6727)\ (z + 0.06539)}{z^2\left(z^2 + 0.382z + 0.04979\right)}\ . \qquad (41)$$

Next, let us deal with the FROH case. Since it turns out that

$$\left|\Theta\left(\mathrm{j}\omega_{\mathrm{d}}\right)\right| = 1.40379\,, \qquad (42)$$

recalling (15) and (21)–(24) we seek a β such that

$$M^2 = \left|\Psi\left(\mathrm{j}2.59808\right)\right|^2 = \frac{1}{\left(1.40379\right)^2} = 0.50745\,. \qquad (43)$$

Now (17) takes the form

$$1.5179\beta^2 + 2.10989\beta + 0.492546 = 0\,, \qquad (44)$$

whose roots are

$$\begin{cases} \beta_1 = -0.274614 \\ \beta_2 = -1.55722\ . \end{cases} \qquad (45)$$

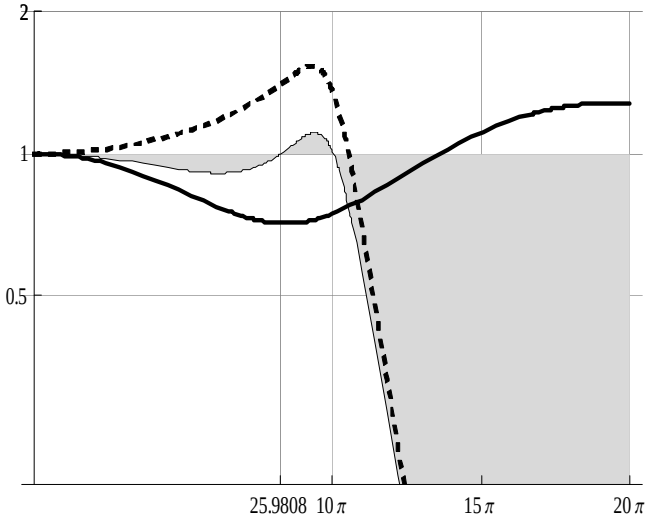

Figure 8. |Θ| (dashed), |ψ| (thick) and |Θψ| (filled) for β_1.

Figs. 8 and 9 show |Θ|, |ψ| as well as their product, all versus ω, for β_1 and β_2 respectively. Both figures show that |Θ| = 1.40379 and |Θψ| = 1 at ω_d. Likewise, Figs. 10 and 11 show the corresponding phase responses. Like in sec. 3.1, β_1 intoduces a small phase lead at ω_d, whereas

β_2 introduces a significant phase lag at ω_d; in view of this, we will take $\beta = \beta_1$ again.

Then, the resulting relevant expressions are:

$$[GG_{\text{FROH}}](z) = \frac{0.00026873(z+6.37)(z+0.50)(z+0.23)(z+0.10)}{z(z-1)(z^3-1.7449z^2+0.8776z+0.1367)} \tag{46}$$

$$\begin{cases} R_{\text{FROH}}(z) = z^4 + 2.63z^3 + 1.69z^2 + 0.35z + 0.02 \\ S_{\text{FROH}}(z) = 1857z^4 - 2377z^3 + 1022z^2 - 145z \\ T_{\text{FROH}}(z) = 356.5964z^4 \end{cases} \tag{47}$$

$$H_{\text{FROH}}(z) = 0.095828\frac{(z+6.37)(z+0.50)(z+0.23)(z+0.10)}{z^3(z^2+0.382z+0.04979)} \tag{48}$$

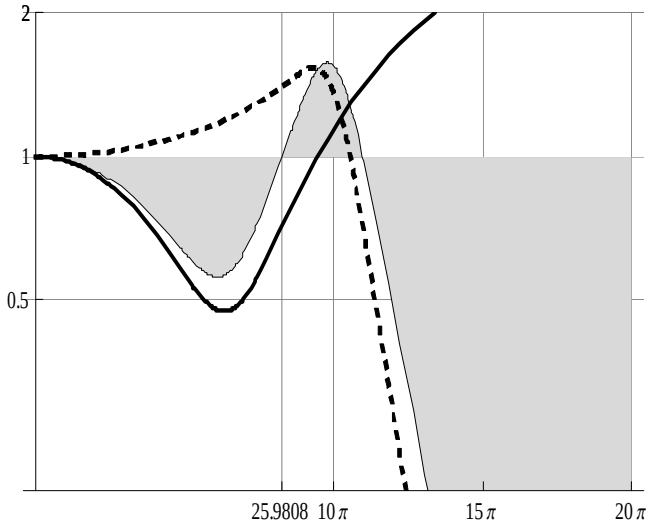

Figure 9. |Θ| (dashed), |ψ| (thick) and |Θψ| (filled) for β_2.

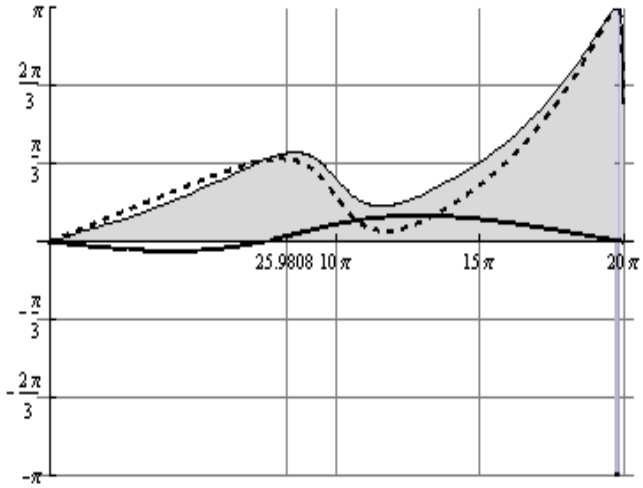

Figure 10. Phase responses corresponding to Fig. 8.

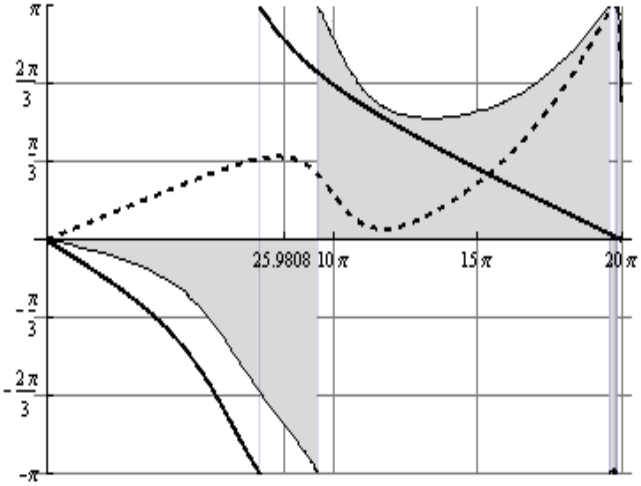

Figure 11. Phase responses corresponding to Fig. 9.

Fig. 12 (plant input) and Fig. 13 (plant output) show the step responses of the three cases studied. Table 2 shows some usual performance figures, such as settling time (5% criterion), overshoot and energy consumed during the transient.

Table 2 makes it clear that the FROH again delivers better performance that the ZOH, not only in terms of the preformance figures, but also considering the continuous-time output. Indeed, Figure 13 shows that the output signal corresponding to the FROH case has a much smoother continuous-time response, as was the case in Sec. 3.1, because, once more, the intersample values tend to lie between the at-sample values.

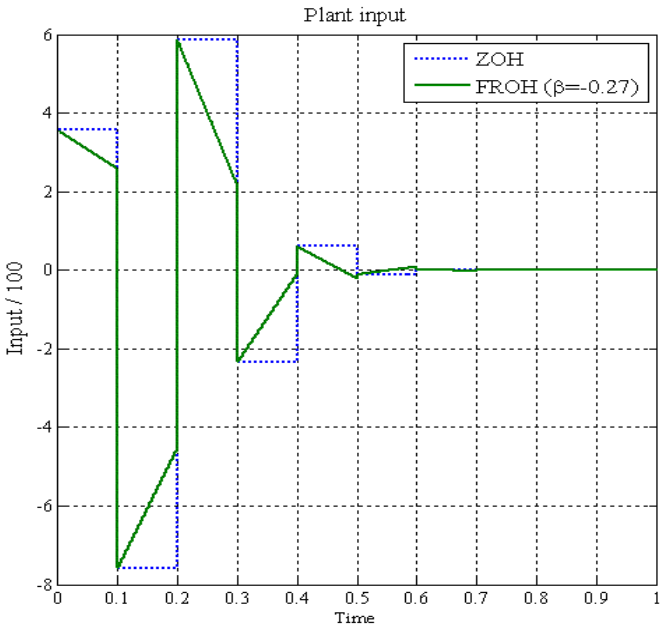

Figure 12. Plant input. ZOH (dotted), FROH (solid).

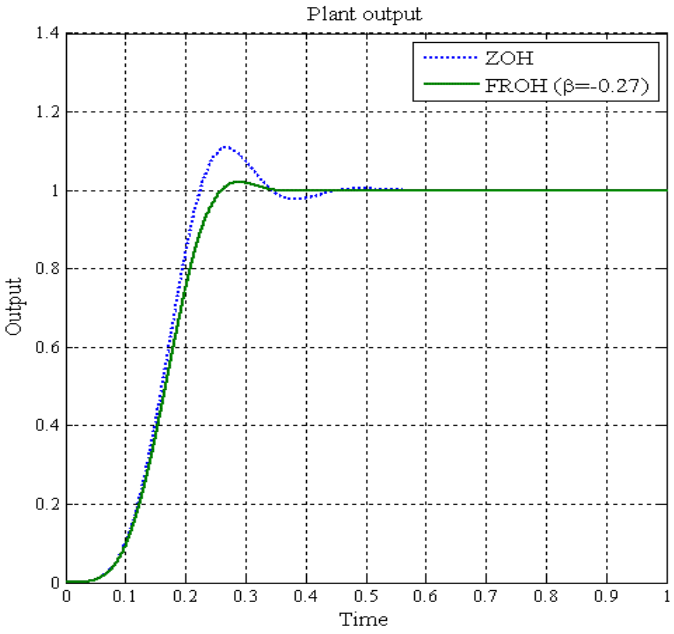

Figure 13. Plant output. ZOH (dotted), FROH (solid).

Figure	ZOH	FROH
$t_{s,5\%}$	313 ms	239 ms
OS	10.89%	2.07%
Energy	110314	66140

Table 2. Significant performance figures.

4 Conclusions

This work has presented a new tuning method for fractional-order hold (FROH) devices operating within sampled-data control systems. It is formulated in the frequency domain, thus it captures the closed-loop intersample behaviour, while avoiding the unwieldy procedure of going through *z*-domain zero placement, which other methods do. Basically, it takes advantage of the ability that the FROH, via its scalar gain β, has to shape a well-known function that describes how apart the continuous-time and the discrete-time responses are in closed-loop. Two application examples have shown that the new method yields clear improvements, not only in terms of step response performance figures such as overshoot, settling time and energy consumed, but also in the intersample behaviour.

5 Acknowledgements

This work has been partially supported by the University of the Basque Country (EHU), Project UPV05/118, and the Basque Government, Project Saiotek-PE05UN09.

References:

[1] K.J. Åström, P. Hagander, J Sternby, Zeros of sampled systems, *Automatica*, Vol. 20, No. 1, 1984, pp. 31-38.

[2] K.J. Åström, B. Wittenmark, *Computer-Controlled Systems*, Prentice Hall, 1997.

[3] R. Bárcena, M. de la Sen, I. Sagastabeitia, DC Motor Digital Control Using a Fractional Order Hold, *Proc. 3rd World Conf. on Circuits, Systems, Communications and Computers, IEEE/CSCC'99*, July 1999, Athens, Greece.

[4] R. Bárcena., M. de la Sen, I. Sagastabeitia, Improving the Stability Properties of the Zeros of Sampled Systems with Fractional Order Hold, *IEE Proc. Control Theory Appl.*, Vol. 147, No. 4, 2000, pp. 456-464.

[5] R. Bárcena, M. de la Sen, A. J. Garrido, Autotuning of Fractional Order Hold Circuits for Digital Control Systems, *Proc. of the 2001 IEEE Int. Conf. on Control Applications*, 2001, pp. 7-12, Mexico City, Mexico.

[6] R. Bárcena, M. de la Sen, I. Sagastabeitia, J.M. Collantes, Discrete Control for a Computer Hard Disc by Using a Fractional Order Hold Device, *IEE Proc. Control Theory Appl.*, Vol. 148, No. 3, 2001, pp. 117-124.

[7] R. Bárcena, A. Etxebarria, U. Ugalde, Optimal Adjustment of Fractional-order Hold Circuits, *Proceedings of the 27th IASTED International Conference*, pp. 184-189, 2008, Innsbruck, Austria.

[8] K. Basterretxea, R. Bárcena, Configurable Digital Fractional Order Hold Device for Hybrid Control Systems, *Proceedings of the 12th WSEAS International Conference on Circuits*, pp. 356-361, 2008, Crete, Greece.

[9] Jianfu Du, Yaou Zhang, Tiansheng Lü, Unmanned Helicopter Flight Controller Design by Use of Model Predictive Control, *WSEAS Transactions on Systems*, Vol. 7, No. 2, pp. 81-87.

[10] G.F. Franklin, J.D. Powell, M.L. Workman, *Digital Control of Dynamic Systems*, Addison-Wesley, 1998.

[11] G.C. Goodwin, S.F. Graebe, M.E. Salgado, *Control Systems Design*, Prentice Hall, 2001.

[12] M. Ishitobi, Stability of Zeros of Sampled Systems with Fractional Order Hold, *IEE Proc. Control Theory Appl.*, Vol. 143, No. 3, 1996, pp. 296-300.

[13] I.D. Landau, G. Zito, *Digital control systems: design, identification and implementation*, Springer, 2006.

[14] Seung Woo Lee, Jun Yeob Song, Construction and Operation of a Knowledge Base on Intelligent Machine Tools, *WSEAS Transactions on Systems*, Vol. 7, No. 3, pp. 148-155.

[15] K.M. Passino, P.J. Antsaklis, Inverse Stable Sampled Low-pass Systems, *Int. J. Control*, Vol. 47, No. 6, 1988, pp. 1905-1913.
[16] Kong Yigang, Wang Zhixin, Optimal Power Capturing of Multi-MW Wind Generation System, *WSEAS Transactions on Systems*, Vol. 7, No. 3, pp. 125-132.
[17] E. Zafiriou, M. Morari, Digital Controllers for SISO Systems: a Review and a New Algorithm, *Int. J. Control*, Vol. 46, No. 4, 1985, pp. 855-876.